A&A 468, 785–795 (2007)
DOI: 10.1051/0004-6361:20066701

Astronomy & Astrophysics

The double Compton emissivity in a mildly relativistic thermal plasma within the soft photon limit

J. Chluba[1], S. Yu. Sazonov[1,2], and R. A. Sunyaev[1,2]

[1] Max-Planck-Institut für Astrophysik, Karl-Schwarzschild-Str. 1, 85741 Garching bei München, Germany
e-mail: jchluba@mpa-garching.mpg.de
[2] Space Research Institute, Russian Academy of Sciences, Profsoyuznaya 84/32, 117997 Moscow, Russia

Received 6 November 2006 / Accepted 20 March 2007

ABSTRACT

Aims. We provide simple and accurate analytic approximations for the low frequency double Compton emission coefficient that are applicable in a broad range of physical situations up to mildly relativistic temperatures. These approximations may be useful for checking in which circumstances the double Compton process is important.

Methods. We perform series expansions of the double Compton emission integral for low energies of the incident photon and electron and compare the derived analytic expressions with the results obtained by numerical integrations of the full double Compton cross section.

Results. We explicitly derived analytic approximations to the low frequency double Compton emission coefficient for initial monochromatic photons and Wien spectra. We show that combining the analytic approximations given in this paper, an accuracy of better than 5% over a very broad range of temperatures and under various physical conditions can be achieved. The double Compton emissivity strongly depends on the ratio of the incoming photon and electron energies: for hard photons and cold electrons the emission is strongly suppressed compared to the case of similar photon and electron energy, whereas in the opposite situation, i.e. hot electrons and soft initial photons, the emission is enhanced. For photons and electrons close to thermodynamic equilibrium the double Compton emissivity increases less rapidly with temperature than in the Lightman-Thorne approximation and the corrections exceed $\sim$10% for temperatures above 4 keV.

Key words. radiation mechanisms: thermal – cosmology: cosmic microwave background – scattering

1. Introduction

Double Compton (DC) scattering is a process of the form $e + \gamma_0 \leftrightarrow e' + \gamma_1 + \gamma_2$. It is related to Compton scattering, like Bremsstrahlung is related to Coulomb scattering of electrons by heavy ions. It corresponds to the lowest order correction in the fine structure constant α to Compton scattering, with *one additional* photon in the outgoing channel, and like thermal Bremsstrahlung it exhibits an *infrared divergence* at low frequencies. In spite of these similarities, in the case of Bremsstrahlung the cross section directly depends on the velocity of the electron relative to the charged particle: there is *no* Bremsstrahlung emission for resting electrons (and ions). On the other hand, for DC scattering the dependence on the velocity of the electron enters only *indirectly* and can be obtained as a result of special relativistic coordinate transformations. Therefore DC emission occurs *whenever* there are photons and free electrons, no matter what the temperature of the electron gas is.

It was realized by Lightman (1981), Thorne (1981) and later by Pozdnyakov et al. (1983) and Svensson (1984) that the DC process in comparison to Bremsstrahlung can become the main source of *soft* photons in astrophysical plasmas with low baryon density and in which magnetic fields are negligible. It has been shown that for given number densities of protons, $N_{\rm p}$, and photons, N_γ, the DC process is expected to dominate over Bremsstrahlung when[1] $N_{\rm p} \lesssim 10 N_\gamma (kT_{\rm e}/m_{\rm e}c^2)^{5/2}$ is fulfilled. This implies that due to the large entropy of the Universe (there are $\sim 1.6 \times 10^9$ photons per baryon), at early stages (redshifts $z \gtrsim 5 \times 10^5$, i.e. at temperatures higher than $\sim 10^6$ K), the DC process becomes very important for the thermalization of possible spectral distortions of the cosmic microwave background (CMB) and the evolution of chemical potential distortions after any significant release of energy in the early Universe (Sunyaev & Zeldovich 1970; Illarionov & Sunyaev 1975a,b; Danese & de Zotti 1982; Burigana et al. 1991; Hu & Silk 1993b). Other possible environments in which the DC process could be of some importance might be found inside the sources of γ-ray bursts or two temperature accretion disks in the vicinity of black holes, both in close binary systems and active galactic nuclei. Given the relevance of DC emission as a source of soft photons within the context of the thermalization of CMB spectral distortions and hard X-ray sources, it is important to investigate the validity of the approximations usually applied to describe the DC process.

Expressions describing DC emission in an *isotropic, cold* plasma and for low energy initial photons, i.e. small $\omega_0 = h\nu_0/m_{\rm e}c^2$, where ν_0 is the frequency of the initial photon γ_0, were first derived by Lightman (1981) and independently by Thorne (1981) within the *soft photon limit*. In this approximation it is assumed that one of the outgoing photons (γ_1 or γ_2) is *soft* compared to the other. Under these assumptions the DC cross section increases $\propto \omega_0^2$ with photon energy (see Jauch & Rohrlich 1976, Eqs. (11)–(45)) and the DC emissivity for broad initial photon distributions is proportional to the integral $I \sim \int \nu_0^4 n(\nu_0)[1 + n(\nu_0)]\,{\rm d}\nu_0$, where here $n(\nu)$ is the photon

[1] For this estimate it was assumed that the incident photons are distributed according to a Wien spectrum with effective temperature $T_{\rm e} \equiv T_\gamma$ and that the plasma is neutral, $N_{\rm e} \equiv N_{\rm p}$.

occupation number (Lightman 1981). We give more details about the Lightman-Thorne approximation in Sect. 2.2.

Again presuming cold electrons and low energy incident photons but making a priori no assumption about the emitted photon energy, Gould (1984) obtained an analytic correction factor for the DC emission coefficient of monoenergetic initial photons, which extends the Lightman-Thorne approximation beyond the soft photon limit. Here the corrections are directly related to the increase of the emitted photon energy (up to energies $\sim\nu_0/2$), while the low frequency emission spectrum remains unchanged.

However, when the temperature of the electrons increases or when the energy of the incident photons grows, one expects corrections to become important, an aspect that has not been included in either of the aforementioned approaches. The corrections due to motion of the electron can be obtained starting with a resting electron in an anisotropic radiation field and then performing the corresponding transformations into the frame where the electron is moving. In contrast to this, the dependence on the energy of the incident photon is related to the exact formulae for the DC cross section as computed using the general theory of quantum-electrodynamics. Here we treat the electron-photon interaction due to DC scattering quantum-electrodynamically for moving electrons and perform all the computations directly in the lab frame, where the photon and electron distributions are assumed to be isotropic.

Temperature corrections to the low frequency DC emissivity for an incoming Wien spectrum, again within the soft photon limit, were discussed by Svensson (1984). It was shown that in the mildly relativistic case the low frequency DC emissivity increases significantly slower with temperature than in the Lightman-Thorne approximation. However, Svensson (1984) only treated one specific case and a more general extension of the Lightman-Thorne approximation is still missing.

In this paper we wish to extend the Lightman-Thorne approach to cases $h\nu_0 \lesssim m_e c^2$ and $kT_e \lesssim m_e c^2$ for isotropic initial photon distributions, but still within the *soft photon limit*. In addition, we will focus on situations when DC *absorption* and *stimulated emission* are negligible. The extension to cases when $\omega_2 \sim \omega_0$ and a discussion of the full kinetic equation for the DC process will be left for a future work. We study the DC emission integral both numerically and analytically and derive approximations to the DC emission coefficient, which are valid in a very broad range of physical situations up to mildly relativistic temperatures. We show that the DC emission coefficient can be expressed in terms of the Lightman-Thorne emission coefficient times a corrections factor, which can be regarded as very similar to the Bremsstrahlung Gaunt-factor, although it has a completely different physical nature. As an example, in Fig. 4 we summarize the results for this low frequency DC correction factor in the case of monochromatic initial photons. One can see that the Lightman-Thorne approximation is accurate in a very limited range of photon energies and electron temperatures. We also investigate the range of applicability of our approximations for initial Wien spectra (Sect. 4.3).

In the following we use $h = c = k = 1$.

2. DC emission for monochromatic photons and thermal electrons in the soft photon limit

In this section we give a detailed derivation of the approximations describing the DC emission for monochromatic initial photons and thermal electrons within the soft photon limit. In particular, we provide some additional comments on the Lightman-Thorne approximation (Sect. 2.2) and introduce a DC correction factor (Sect. 2.3) relative to the Lightman-Thorne formula which will be used in the following. See Table 1 for overview.

2.1. General formulation

DC emission is a result of the interaction between an electron and a photon with *one* additional photon in the outgoing channel:

$$e(P) + \gamma(K_0) \longrightarrow e(P') + \gamma(K_1) + \gamma(K_2)\,.$$

Here $P = (E, \boldsymbol{p})$, $P' = (E', \boldsymbol{p}')$ and $K_i = (\nu_i, \boldsymbol{k}_i)$ denote the corresponding particle four-momenta[2]. The full DC scattering squared matrix element and differential cross sections for various limiting cases were first derived by Mandl & Skyrme (1952) and may also be found in Jauch & Rohrlich (1976).

In this section we focus our analysis only on the emission process for *isotropic, monochromatic* initial photons, with phase space density $n(\nu) = N_0\,\delta(\nu-\nu_0)/\nu_0^2$, and *isotropic, thermal* electrons of temperature T_e. Above N_0 in physical units is defined by $N_{\gamma,0} = 8\pi\,N_0/c^3$, where $N_{\gamma,0}$ is the photon number density. In this case the change of the photon phase space density, $n_2 = n(\nu_2)$, at frequency ν_2 due to DC emission can be written as

$$\left.\frac{\partial n_2}{\partial t}\right|_{\rm em}^{\rm m} = \frac{N_0}{\nu_2^2}\int {\rm d}^3p \int {\rm d}\Omega_0 \int {\rm d}\Omega_1\, g_0 \frac{{\rm d}\sigma_{\rm DC}}{{\rm d}\Lambda} f. \tag{1}$$

Here the DC differential cross section (cf. Jauch & Rohrlich 1976, Eqs. (11)–(38)) is given by

$$\frac{{\rm d}\sigma_{\rm DC}}{{\rm d}\Lambda} = \frac{\alpha\, r_0^2}{(4\pi)^2}\frac{\nu_1\,\nu_2}{g_0\gamma\,\nu_0}\frac{X}{(P + K_0 - K_2)\cdot\hat{K}_1}\,, \tag{2}$$

where X may be found in the Appendix B and we defined the *Møller relative speed* of the incident electron and photon as $g_i = \hat{P}\cdot\hat{K}_i = 1 - \beta\,\mu_{ei}$, with the dimensionless electron velocity $\beta = |\boldsymbol{v}|/c = |\hat{\boldsymbol{p}}| = |\boldsymbol{p}|/E$ and the directional cosine[3] $\mu_{ei} = \hat{\boldsymbol{p}}\cdot\hat{\boldsymbol{k}}_i$. Furthermore $\alpha = e^2/4\pi \approx 1/137$ is the fine structure constant, $r_0 = \alpha/m_e \approx 2.82\times10^{-13}$ cm is the classical electron radius and $\gamma = \sqrt{1-\beta^2}$ denotes the Lorentz-factor of the initial electron.

In Eq. (1) we have neglected induced effects, i.e. we assumed $N_0 \ll \nu_0^2$ and that the electrons are non-degenerate. The latter simplification, for sufficiently low temperatures and electron densities (such as in the Universe for $T_e \lesssim m_e$), is justified, but as we will discuss in Sect. 3.2, for broad initial photon distributions, stimulated DC emission can become important. However, a full treatment of this problem is much more complicated and is beyond the scope of this paper. The electron phase space density may be described by a relativistic Maxwell-Boltzmann distribution

$$f(E) = \frac{N_e}{4\pi\, m_e^3\, K_2(1/\theta_e)\,\theta_e}\,{\rm e}^{-E/m_e\theta_e}\,, \tag{3}$$

where $K_2(1/\theta_e)$ is the modified Bessel function of the second kind (Abramovitz & Stegun 1965), with $\theta_e = T_e/m_e$, and where N_e is the electron number density, such that $N_e = \int f(E)\,{\rm d}^3p$. In the low temperature limit ($\theta_e \ll 1$) the relativistic Maxwell Boltzmann distribution (3) can be handled by the expression

[2] Henceforth bold font denotes 3-vectors.

[3] Note that in the following an additional hat above 3- and 4-vectors indicates that they are normalized to the time-like coordinate of the corresponding 4-vector.

given in Appendix A, which is useful for both analytic and numerical purposes.

In general the DC emission integral (1) has to be performed numerically. Some comments on the numerical approach we use to solve the multidimensional Boltzmann integrals is given in Appendix C. However, in the limit of low temperatures and energies of the initial photon it is possible to derive various useful analytic approximations, which we discuss in the following. In practice we obtained the numerical results for the soft photon limit by setting the frequency of the emitted photon to a very small value as compared to the incident photon energy ($\nu_2 \sim \nu_0 \times 10^{-4}$).

2.2. Lightman-Thorne approximation

The expression for DC emission from monoenergetic initial photons and cold electrons as given by Lightman (1981) and independently by Thorne (1981) can be deduced from the emission integral (1) by performing a series expansion of the DC differential cross-section (2) in lowest orders of $\nu_0 \ll m_e$ and $\nu_2 \ll m_e$ and setting $\beta = 0$, i.e. assuming that the electrons are initially at rest. In this limit $f(p) = N_e\, \delta(p)/4\pi p^2$ and the integration over d^3p can be carried out immediately.

The series expansion in lowest order of $\nu_2 \ll m_e$ is equivalent to using the *soft photon approximation* for the DC differential cross section, i.e. assuming in addition that $\nu_2 \ll \nu_0$. Due to energetic arguments the scattered photon frequency has to be close to the initial photon frequency ($\nu_1 \sim \nu_0$). Therefore the *infrared divergence* due to the integration over the phase space volume for the photon γ_1 is automatically avoided. In the following we use the notations $\mu_{ij} = \hat{\boldsymbol{k}}_i \cdot \hat{\boldsymbol{k}}_j$ and ϕ_{ij} for the directional cosines and azimuthal angles between the photons i and j, respectively. It then follows:

$$\left.\frac{d\sigma_{DC}^{soft}}{d\Lambda}\right|_L \approx \frac{\alpha}{4\pi^2}\, r_0^2\, \frac{\omega_0^2}{\nu_2}\, [1+\mu_{01}^2]\left[1-\mu_{01}-\frac{\Delta\mu^2}{2}\right], \quad (4)$$

with $\Delta\mu = \mu_{02} - \mu_{12}$. Furthermore we have introduced the dimensionless photon energy $\omega_i = \nu_i/m_e$.

Now, after aligning the z-axis with the direction of the emitted photon all the integrations can be easily performed analytically. Making use of the identity $\mu_{01} = \mu_{02}\,\mu_{12} + \cos(\phi_{02}-\phi_{12})(1-\mu_{02}^2)^{1/2}(1-\mu_{12}^2)^{1/2}$, where ϕ_{02} and ϕ_{12} denote the azimuthal angles of the initial and the scattered photon, respectively, this leads to the *Lightman-Thorne* approximation for the DC emission spectrum of cold electrons and soft, monochromatic initial photons

$$\left.\frac{\partial n_2}{\partial t}\right|_{em,L}^{m} = \frac{4\alpha}{3\pi}\, N_e\, N_0\, \sigma_T\, \frac{\omega_0^2}{\nu_2^3}, \quad (5)$$

with the *Thomson* scattering cross section $\sigma_T = 8\pi r_0^2/3 \approx 6.65 \times 10^{-25}$ cm^2. The expression (5) is the DC scattering equivalent of the *Kramers* formula for thermal Bremsstrahlung. The characteristics of Eq. (5) can be summarized as follows: the DC emission spectrum increases $\propto \omega_0^2$ and, as mentioned earlier, exhibits an *infrared* divergence for $\nu_2 \to 0$. It is usually assumed that under physical conditions inside an astrophysical plasma, emission and absorption balance each other below some frequency, $\nu_{2,min}$, and that energy conservation in addition introduces some high frequency cutoff, $\nu_{2,max}$. Therefore the photon production rate increases logarithmically,

$$\left.\frac{\partial N_2}{\partial t}\right|_{em,L}^{m} = \frac{4\alpha}{3\pi}\, N_e\, N_0\, \sigma_T\, \omega_0^2 \times \ln\left(\frac{\nu_{2,max}}{\nu_{2,min}}\right), \quad (6)$$

with the ratio of the upper to the lower frequency cutoff of the DC emission spectrum.

It is obvious that due to the DC process the interacting electrons and high frequency photons can lose some part of their energy due to the emission of soft photons. However, in the majority of applications the energy losses connected with Compton heating and cooling are much larger.

As will be discussed in more detail below, the Lightman-Thorne approximation only describes the low frequency part of the DC emission spectrum for cold electrons and soft initial photons ($\nu_0/m_e \le 10^{-3}$) well. For initial photons with slightly higher energies, next order terms lead to a significant suppression of the emission at low frequencies relative to the Lightman-Thorne approximation (see Fig. 1 and the discussion in Sect. 2.4).

Table 1. Analytic approximations for the DC correction factor (7) relative to the Lightman-Thorne formula as obtained in Sect. 2. Within the quoted range of applicability each approximation should be accurate to better than ~5%. However, for $G_m^{inv}(\omega_0, \theta_e) = \left\langle G_m^{inv}\right\rangle_{th}$ as based on Eqs. (14) and (16) we refer the reader to Fig. 4.

Symbol	Reference	Range	Comment
$G_m^0(\omega_0)$	Eq. (8), Fig. 1	$\theta_e = 0$, $\omega_0 \lesssim 0.15$	expansion
$G_m^{0,inv}(\omega_0)$	Eq. (9), Fig. 1	$\theta_e = 0$, $\omega_0 \lesssim 1$	inv. factor
$G_m^{nr}(\theta_e)$	Eq. (12), Fig. 2	$\theta_e \lesssim 1$, $\omega_0 \ll 1$	expansion
$G_m^{nr}(\theta_e)$	Eq. (12b), Fig. 2	$\theta_e \lesssim 0.5$, $\omega_0 \ll 1$	expansion
$G_m(\omega_0, \theta_e)$	Eq. (15), Fig. 3	$\theta_e \lesssim 0.2$, $\omega_0 \lesssim 0.1$	expansion
$G_m^{inv}(\omega_0, \theta_e)$	see above, Fig. 3	Fig. 4	inv. factor

2.3. DC correction factor within the soft photon limit

Below we discuss the numerical and analytical results for the DC emission integral (1). For convenience using Eq. (1) and the Lightman-Thorne approximation (5) we introduce the new function G as

$$G_m(\omega_0, \theta_e) = \frac{\partial_t n_2|_{em}^{m}}{\partial_t n_2|_{em,L}^{m}} \quad (7)$$

in order to compare the different cases. This function can be regarded as very similar to the Bremsstrahlung *Gaunt* factor, although it has a different physical origin. Deviations of G from unity are directly related to DC higher order corrections in the energies of the initial photons and electrons.

2.4. Cold electrons and energetic initial photons

We expand the DC differential cross section (2) in the lowest order of $\omega_2 = \nu_2/m_e$ and setting $\beta = 0$. Then we expand the resulting expression up to 4th order in ω_0 to take into account higher order corrections in the energy of the initial photon. Carrying out all the integrations in the emission integral (1) yields the correction factor $G_m^0(\omega_0)$ following from the *direct* series expansion:

$$G_m^0(\omega_0) = 1 - \frac{21}{5}\,\omega_0 + \frac{357}{25}\,\omega_0^2 - \frac{7618}{175}\,\omega_0^3 + \frac{21498}{175}\,\omega_0^4. \quad (8)$$

Figure 1 shows the full numerical result for $G_m^0(\omega_0)$ in comparison to the analytic approximation (8), taking into account the corrections up to different orders in ω_0. The approximation converges only very slowly and in the highest order considered here it breaks down close to $\omega_0 \sim 0.15$. Due to this behavior of the asymptotic expansion one expects no significant improvement when going to higher orders in ω_0, but the monotonic decrease of the emission coefficient suggests that a functional form

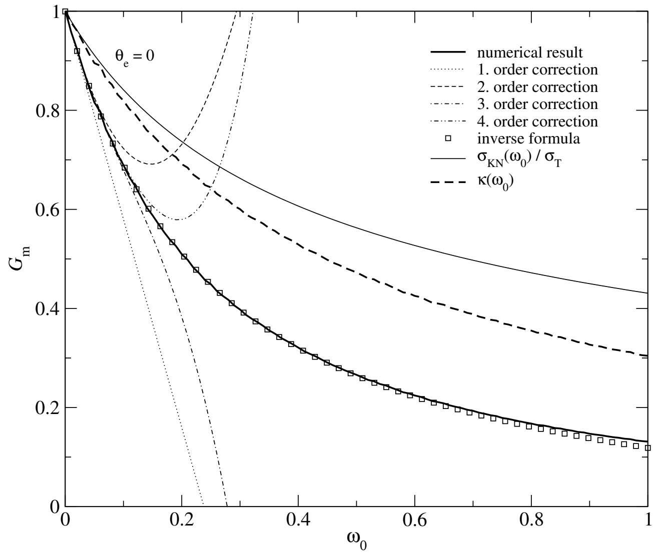

Fig. 1. DC emission correction factor $G^0_{\rm m}$ for cold electrons and monochromatic initial photons as a function of $\omega_0 = \nu_0/m_{\rm e}$. Also shown are the *direct* expansion (8), up to different orders in ω_0, and the *inverse* approximation (9). For comparison, we also show the frequency dependence of the total Compton cross section, $\sigma_{\rm KN}$, as given by the *Klein-Nishina* formula and the correction factor $\kappa(\omega_0) = G^0_{\rm m}/(\sigma_{\rm KN}/\sigma_{\rm T})$ per act of Compton scattering.

$G^0_{\rm m} = [1 + \sum_{k=1}^4 a_k\,\omega_0^k]^{-1}$ could lead to a better performance. Determining the coefficients a_i by comparison with the direct expansion (8) one may obtain an *inverse* approximation for the DC correction factor

$$G^{0,\rm inv}_{\rm m}(\omega_0) = \frac{1}{1 + \frac{21}{5}\,\omega_0 + \frac{84}{25}\,\omega_0^2 - \frac{2041}{875}\,\omega_0^3 + \frac{9663}{4375}\,\omega_0^4}. \tag{9}$$

As Fig. 1 clearly shows, $G^{0,\rm inv}_{\rm m}(\omega_0)$ provides an excellent description of the numerical result up to very high energies of the initial photon. For comparison, we also show the frequency dependence of the total Compton cross section, $\sigma_{\rm KN}$, as given by the *Klein-Nishina* formula and the correction factor $\kappa(\omega_0) = G^0_{\rm m}/(\sigma_{\rm KN}/\sigma_{\rm T})$ per act of Compton scattering. Since it is expected that per *single* Compton scattering a small fraction of electrons and photons undergo DC scattering, this comparison hints towards the fact that a large part ($\sim$2/3) of the decrease in the DC emissivity with ω_0 is due to the decrease in the probability of Compton scattering photons with larger energies due to quantum-electrodynamic corrections.

2.5. Hot electrons and soft initial photons

We now consider the limit $\nu_0 \ll m_{\rm e}$ and $\nu_2 \ll \nu_0$. Expanding the DC differential cross section (2) in the lowest orders of ν_0 and ν_2 one obtains

$$\frac{{\rm d}\sigma^{\rm soft}_{\rm DC}}{{\rm d}\Lambda} \approx \frac{\alpha}{2\pi^2}\,\frac{r_0^2}{g_0}\,\frac{\omega_0^2}{\nu_2}\left[\gamma^2\lambda_0\lambda_1(\gamma^2\lambda_0\lambda_1 - \alpha_{01}) + \frac{\alpha_{01}^2}{2}\right] \times \frac{\gamma^2\lambda_0\lambda_1\lambda_2^2\alpha_{01} - \frac{1}{2}(\lambda_1\alpha_{02} - \lambda_0\alpha_{12})^2}{\gamma^{10}\lambda_0\lambda_1^6\lambda_2^4} \tag{10}$$

with the electron and photon scalars $\lambda_i = \hat{P}\cdot\hat{K}_i = 1 - \beta\mu_{ei}$ and $\alpha_{ij} = \hat{K}_i\cdot\hat{K}_j = 1 - \mu_{ij}$. Now we perform all the angular integrations of the Boltzmann emission integral (1) but assume monoenergetic electrons, with velocity β_0. This then leads to

$$\left.\frac{\partial n_2}{\partial t}\right|^{\rm m,nr}_{\rm em} = \frac{1+\beta_0^2}{1-\beta_0^2} \times \left.\frac{\partial n_2}{\partial t}\right|^{\rm m}_{\rm em,L}. \tag{11}$$

Here the factor of γ_0^2 can be immediately understood since the initial photons inside the rest frame of the electron will on average have an energy of $\omega_0^{\rm e} \sim \gamma_0\omega_0$ and hence the DC emissivity, i.e. $\propto(\omega_0^{\rm e})^2$, will be $\sim\gamma_0^2$ times larger than for resting electrons.

From Eq. (11) the correction factor for thermal electrons with temperature $\theta_{\rm e}$ can be found by averaging over the relativistic Maxwell-Boltzmann distribution (3):

$$G^{\rm nr}_{\rm m}(\theta_{\rm e}) = \int_0^\infty \frac{1+\beta_0^2}{1-\beta_0^2}\,f(E_0)\,p_0^2\,{\rm d}p_0 \equiv 2\left\langle\gamma_0^2\right\rangle_{\rm th} - 1$$

$$= \frac{[1 + 24\,\theta_{\rm e}^2]\,K_0(1/\theta_{\rm e}) + 8\,\theta_{\rm e}\,[1 + 6\,\theta_{\rm e}^2]\,K_1(1/\theta_{\rm e})}{K_2(1/\theta_{\rm e})} \tag{12a}$$

with $E_0 = \gamma_0 m_{\rm e}$, $p_0 = \gamma_0 m_{\rm e}\beta_0$ and $\gamma_0 = (1-\beta_0^2)^{-1/2}$. Here $K_i(1/\theta_{\rm e})$ denotes a modified Bessel function of kind i. For low temperatures one can find the approximation

$$G^{\rm nr}_{\rm m}(\theta_{\rm e}) \overset{\theta_{\rm e}\ll 1}{\approx} 1 + 6\,\theta_{\rm e} + 15\,\theta_{\rm e}^2 + \frac{45}{4}\,\theta_{\rm e}^3 - \frac{45}{4}\,\theta_{\rm e}^4. \tag{12b}$$

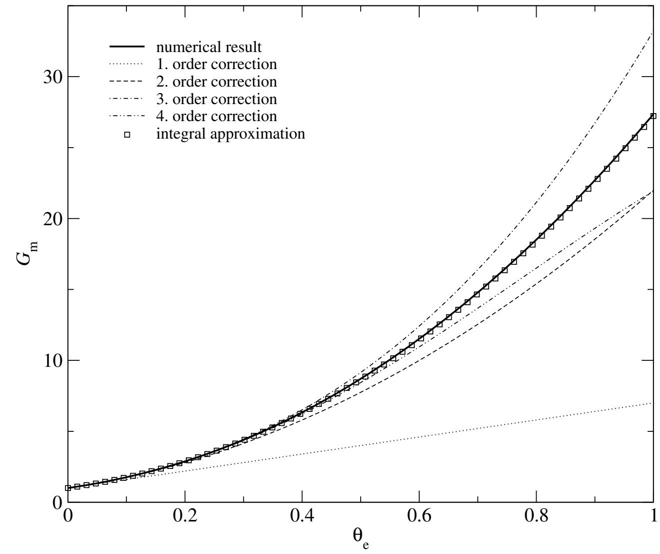

Fig. 2. DC emission correction factor $G^{\rm nr}_{\rm m}$ for soft initial photons ($\omega_0 = 10^{-4}$) as a function of the electron temperature $\theta_{\rm e} = T_{\rm e}/m_{\rm e}$. Also shown is the full integral approximation (12a) and the expansion (12b), taking into account the corrections up to different orders in $\theta_{\rm e}$, as indicated.

Figure 2 shows the numerical result for $G^{\rm nr}_{\rm m}$ in comparison with the analytic approximations (12). The low frequency DC emission strongly increases with temperature. One can gain a factor of a few for $\theta_{\rm e} \le 0.5$ and even a factor $\sim$30 for $\theta_{\rm e} \sim 1$. The expansion (12b) provides an excellent description of the numerical results up to high temperatures ($\theta_{\rm e} \sim 0.5$), but for higher temperatures the integral approximation (12a) should be used.

2.6. Hot electrons and energetic initial photons

To improve the analytic description of the DC emission we again return to the soft photon limit, expanding the DC differential cross section (2) in the lowest orders of $\nu_2 \ll m_{\rm e}$. To include higher order corrections we also expand this expression up to 4th order in ω_0. We then carry out all the angular integrations of the Boltzmann emission integral (1) for monoenergetic electrons, with velocity β_0. This leads to

$$\begin{aligned} G_\mathrm{m}(\omega_0,\beta_0) \;=\; \gamma_0^2\Bigg[& 1+\beta_0^2-\frac{21}{5}\left(1+2\beta_0^2+\frac{1}{5}\beta_0^4\right)\gamma_0\omega_0 \\ & +\frac{357}{25}\left(1+\frac{10}{3}\beta_0^2+\beta_0^4\right)\gamma_0^2\omega_0^2 \\ & -\frac{7618}{175}\left(1+5\beta_0^2+3\beta_0^4+\frac{1}{7}\beta_0^6\right)\gamma_0^3\omega_0^3 \\ & +\frac{21498}{175}\left(1+7\beta_0^2+7\beta_0^4+\beta_0^6\right)\gamma_0^4\omega_0^4\Bigg]. \end{aligned} \tag{13}$$

As in the previous case the correction factor for thermal electrons with temperature θ_e can be found by performing the 1-dimensional integral

$$\langle G_\mathrm{m}\rangle_\mathrm{th} \equiv G_\mathrm{m}(\omega_0,\theta_\mathrm{e}) = \int_0^\infty G_\mathrm{m}(\omega_0,\beta_0)\, f(E_0)\, p_0^2\,\mathrm{d}p_0\,. \tag{14}$$

Unfortunately here no full solution in terms of simple elementary functions can be given, but the integral can be easily evaluated numerically. In the limit of low temperatures one can find the simple approximation

$$\begin{aligned} G_\mathrm{m}(\omega_0,\theta_\mathrm{e}) \;\approx\; & 1-\frac{21}{5}\,\omega_0+\frac{357}{25}\,\omega_0^2-\frac{7618}{175}\,\omega_0^3+\frac{21498}{175}\,\omega_0^4 \\ & +\left[6-\frac{441}{10}\,\omega_0+\frac{5712}{25}\,\omega_0^2-\frac{34281}{35}\,\omega_0^3\right]\theta_\mathrm{e} \\ & +\left[15-\frac{8379}{40}\,\omega_0+\frac{8568}{5}\,\omega_0^2\right]\theta_\mathrm{e}^2 \\ & +\left[\frac{45}{4}-\frac{3969}{8}\,\omega_0\right]\theta_\mathrm{e}^3-\frac{45}{4}\,\theta_\mathrm{e}^4 \end{aligned} \tag{15}$$

for (14), which clearly shows the connection to the two limits discussed above, i.e. Eq. (8) and (12b).

As was shown in Sect. 2.4 an *inverse* Ansatz for G_m led to an excellent approximation for the full numerical result in the cold plasma case. To improve the performance of the obtained analytic approximation for $G_\mathrm{m}(\omega_0,\beta_0)$ we tried many different functional forms, always comparing with the direct expansion (13). After many attempts we found that

$$G_\mathrm{m}^\mathrm{inv}(\omega_0,\beta_0) = \frac{\gamma_0^2\,(1+\beta_0^2)}{1+\sum_{k=1}^4 f_k(\beta_0)\,\gamma_0^k\omega_0^k}\,, \tag{16a}$$

with the functions $f_k(\beta_0)$

$$f_1(\beta_0) \;=\; \frac{1}{1+\beta_0^2}\left[\frac{21}{5}+\frac{42}{5}\beta_0^2+\frac{21}{25}\beta_0^4\right] \tag{16b}$$

$$f_2(\beta_0) \;=\; \frac{1}{(1+\beta_0^2)^2}\left[\frac{84}{25}+\frac{217}{25}\beta_0^2+\frac{1967}{125}\beta_0^4\right] \tag{16c}$$

$$f_3(\beta_0) \;=\; -\frac{1}{(1+\beta_0^2)^3}\left[\frac{2041}{25}+\frac{1306}{125}\beta_0^2\right] \tag{16d}$$

$$f_4(\beta_0) \;=\; \frac{1}{(1+\beta_0^2)^4}\,\frac{9663}{4375} \tag{16e}$$

provides the best description of the full numerical results.

Figure 3 shows the numerical results for $G_\mathrm{m}(\omega_0,\theta_\mathrm{e})$ in comparison with the integral approximation (14) in combination with the inverse factor (16a) and the direct expansion (15) taking into account correction terms up to fourth order. The performance of the integral approximation is excellent in the full range of considered cases, but the direct expansion breaks down at lower and lower temperatures once the initial photon frequency increases. For $\omega_0 \le 0.1$ the direct expansion should be applicable within a few percent accuracy up to $\theta_\mathrm{e} \sim 0.2$.

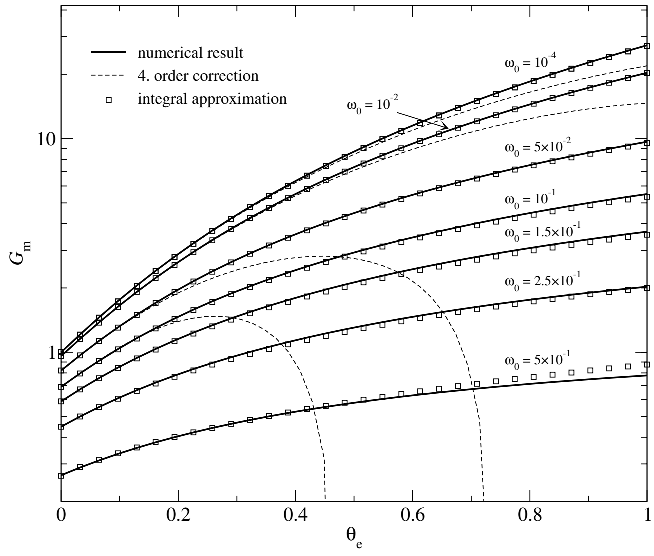

Fig. 3. DC emission correction factor G_m for different energies of the initial photons as a function of $\theta_\mathrm{e} = T_\mathrm{e}/m_\mathrm{e}$. Also shown is the full integral approximation (14) in combination with the inverse factor (16a) and, for some cases, the expansion (15) taking into account correction terms up to fourth order, as indicated.

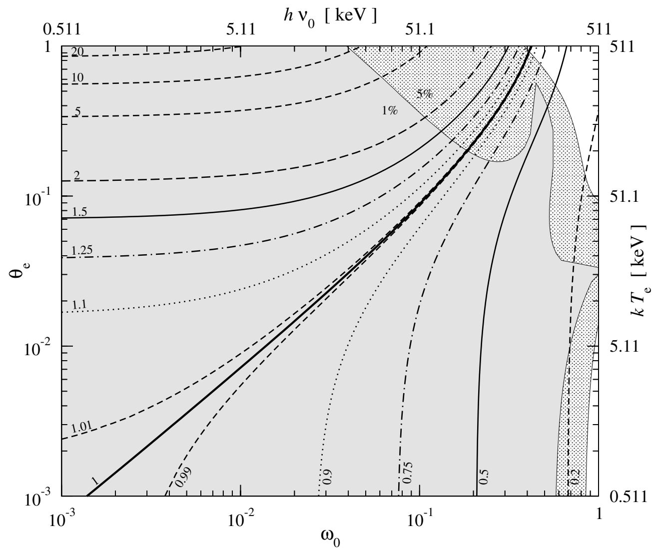

Fig. 4. DC emission correction factor for monoenergetic initial photons and thermal electrons. The lines indicate the contours of G_m = const. as obtained by full numerical integrations. Within the shaded regions the approximation based on (16) is accurate to better than 1% and 5%, respectively.

In Fig. 4 the dependence of the DC emission correction factor on the energy of the initial photons and the temperature of the electrons is illustrated. From this one can see that the Lightman-Thorne approximation is applicable in a very limited range of photon energies and electron temperatures. On the other hand the approximation based on (16) works in practically the full considered range with very high accuracy. Focusing on the curve $G_{\rm m} = 1$ one can see that for low energies of the initial photon ($\omega_0 \lesssim 10^{-2}$) the required electron temperature scales like $\theta_{\rm e} \sim 0.7\,\omega_0$. Considering the first order correction terms in Eq. (15) one also finds this scaling. Up to $\omega_0 \gtrsim 0.15$ the necessary temperature of the electrons is $\theta_{\rm e} < \omega_0$. This shows that moving electrons can easily compensate the suppression of DC emission due to the increasing energy of the initial photon. However, for $\omega_0 \gtrsim 0.15$ the electrons have to be up to several times hotter to accomplish this.

3. DC emission for more general initial photon distributions

Based on the results given in the previous Section one can obtain simple expressions for more general initial photon distributions. For initial photons with phase space distribution $n(\nu)$ within the *Lightman-Thorne approximation* one finds

$$\left.\frac{\partial n_2}{\partial t}\right|^{\rm soft}_{\rm DC,\,em} = \frac{4\alpha}{3\pi}\,N_{\rm e}\,\sigma_{\rm T}\,\frac{\theta_\gamma^2}{x_2^3} \times I_0\,, \tag{17}$$

where here we defined the dimensionless photon frequency $x_i = \omega_i/\theta_\gamma = \nu_i/T_\gamma$. We also introduced the *effective temperature* T_γ which characterizes the total energy density of the photon field. For Planckian photons T_γ is identical with the *thermodynamic temperature*.

The DC emission factor I_0 is given by the integral (compare Lightman (1981), Eq. (10b) for $n(\nu) \ll 1$):

$$I_0 = \int_0^\infty x^4\,n(x)\,{\rm d}x, \tag{18}$$

over the initial photon distribution $n(\nu)$. Stimulated DC emission was neglected, but we will discuss possible extensions in Sect. 3.2. Here one factor of x^2 arises from the conversion $N_0 \to \nu^2 n(\nu)$, and the other is due to the scaling of the *Lightman-Thorne approximation* Eq. (5) with ω_0. Note that here and below we omit the index "0" for the frequency of the initial photon.

Now including higher order corrections in the energies of the initial photon and electrons, but still in lowest order of x_2, instead of I_0 one will obtain a more general function I. With this we can define an *effective DC emission correction factor* in the soft photon limit by

$$g_{\rm dc}^{\rm soft} = I/I_0. \tag{19}$$

We shall now give analytic expressions for I based on the results obtained in the previous section.

3.1. The effective DC emission correction factor

Here we will give analytic expressions for the effective DC emission correction factor with *three different* approaches, each with their advantages and disadvantages. We will discuss the range of applicability for these expressions for Wien spectra in the next section.

3.1.1. Approximation based on $G_{\rm m}^{\rm inv}$

As was shown in Sect. 2.6 the expression (16) averaged over a thermal electron distribution (compare with Eq. (14)) provides an excellent description of the DC emissivity for monochromatic initial photons. If induced effects are negligible one can simply convolve this result with the corresponding initial photon distribution $n(\nu)$ to obtain:

$$I = \int_0^\infty x^4\,n(x)\left\langle G_{\rm m}^{\rm inv}\right\rangle_{\rm th}\,{\rm d}x\,. \tag{20}$$

Here $\left\langle G_{\rm m}^{\rm inv}\right\rangle_{\rm th}$ denotes the thermally averaged expression (16). As will be shown below, the approximation (20) works very well in a broad range of different temperatures. However, it involves a 2-dimensional integral which in numerical applications may be too demanding.

3.1.2. Direct expansion of $G_{\rm m}$

One can also replace $\left\langle G_{\rm m}^{\rm inv}\right\rangle_{\rm th}$ in Eq. (20) with the more simple analytic expression (15) derived in the limit of low electron temperature and energy of the initial photon. In this case the DC emission coefficient I can be written as the *direct* expansion

$$I^{\rm exp} = \sum_{k=0}^{4} I_k \times \theta_{\rm e}^k \tag{21}$$

where the definitions of the integrals I_i may be found in Appendix (C.2). The first integral I_0 corresponds to the result obtained by Lightman (1981) and Thorne (1981) in the limit $n(\nu) \ll 1$. However, it is expected that this approximation in general converges very slowly and is mainly useful for simple analytic estimates.

3.1.3. Alternative approach

Above we gave the expressions obtained from the *direct* expansion of I. However, this procedure results in an asymptotic expansion of the effective DC correction factor $g_{\rm dc}^{\rm soft}$ or equivalently I, which in most of the cases is expected to converge very slowly. Therefore, using the *direct* expansion (21) we again tried to "guess" the correct functional form of the DC emission coefficient I and thereby to extend the applicability of this simple analytic expression. The general behavior of the results obtained in our numerical integrations showed that for $\theta_{\rm e} \lesssim \theta_\gamma$ the effective DC correction factor $g_{\rm dc}^{\rm soft} = I/I_0$ decreases towards higher electron temperatures. After several attempts we found that this behavior is best represented by the functional form

$$I^{\rm inv} = \frac{I_0}{1 + a\,\theta_{\rm e}}\cdot \tag{22a}$$

Using Eq. (21), one finds

$$a = \frac{21}{5}\,\frac{\theta_\gamma}{\theta_{\rm e}}\,\frac{\int x^5\,n\,{\rm d}x}{\int x^4\,n\,{\rm d}x} - 6\,. \tag{22b}$$

As will be shown below, Eq. (22a) together with (22b) provides a description of the low frequency DC emission coefficient, which for photon distributions close to a Wien spectrum is accurate to better than 5% for temperatures up to ~25 keV in the range $0.2 \le \rho \le 50$. Here we defined the ratio of the electron to photon temperature as $\rho = T_{\rm e}/T_\gamma$. For a detailed discussion we refer the reader to Sect. 4.2. Since this approximation involves only 1-dimensional integrals over the initial photon distribution in numerical applications it may be more useful than the approximation (20).

3.2. Approximate inclusion of stimulated DC emission

For broad initial photon distributions, stimulated DC emission arises which, in particular for situations close to full thermodynamic equilibrium, can become significant. Accounting for this effect, the DC emission integral contains additional factors of $1 + n(\nu_1)$ and $1 + n(\nu_2)$ due to the presence of ambient photons at frequencies ν_1 and ν_2. If we are interested in the emission of photons at frequency ν_2 then $1 + n(\nu_2)$ appears as a global factor in front of the full Boltzmann emission integral and no further complications arise due to this term. However, the factor $1 + n(\nu_1)$ remains inside the integrand and the dependence of the scattered photon frequency on the scattering angles and energies has to be taken into account.

Within the Lightman-Thorne approximation, for a particular DC scattering event one always has $\nu_0 \sim \nu_1$, since for $T_e = 0$ no *Doppler boosting* appears and for $\nu_0 \ll m_e$ the *recoil effect* is negligible. Therefore one can write

$$I_0^{\rm stim} \approx [1 + n(x_2)] \times \int_0^\infty x^4\, n(x)[1 + n(x)]\,{\rm d}x \tag{23}$$

instead of Eq. (18). In situations close to full thermodynamic equilibrium the main effect due to stimulated DC emission is *only* due to the factor $1 + n(x_2)$, whereas the correction related to $1 + n(x)$ inside the integral is only of a few percent. Assuming $n(x) = 1/[{\rm e}^x - 1]$ yields $I_0 \sim 24.89$ and $I_0^{\rm stim} \sim 25.98/x_2$ for $x_2 \ll 1$ which further supports this statement.

Similarly, one can modify Eq. (20) with the replacement $n(x) \to n(x)[1 + n(x)][1 + n(x_2)]$, but again this approach is limited to cases when the change of the initial photon energy is very small ($\nu_0 \sim \nu_1$) and the radiation spectrum is broad ($\Delta\nu/\nu \gg \beta$). This then yields

$$I^{\rm stim} \approx [1 + n(x_2)] \times \int_0^\infty x^4\, n(x)[1 + n(x)] \left\langle G_{\rm m}^{\rm inv}\right\rangle_{\rm th} {\rm d}x. \tag{24}$$

Now, looking at the ratio $g_{\rm dc}^{\rm stim} = I^{\rm stim}/I_0^{\rm stim}$ one again expects that due to stimulated processes the effective DC emission correction factor will also be affected at the percent-level only. We confirmed this statement for Planckian initial photons with $T_\gamma = T_e$ performing the full Boltzmann emission integral, but a more detailed treatment of this problem is beyond the scope of this paper, and as mentioned above below we restrict ourselves to cases in which stimulated DC emission is negligible. Furthermore it is clear that in situations when stimulated DC emission becomes important, DC absorption also should be taken into account and a full derivation of the kinetic equation for the evolution of the photon field under the DC process is required. In lowest order and for situations very close to full thermodynamic equilibrium, accounting for higher order corrections in the initial photon energy and electron temperature, one can simply multiply the *kinetic equation* for the time evolution of the photon field under DC scattering as formulated by Lightman (1981) and Thorne (1981), by the effective DC correction factor $g_{\rm dc}^{\rm soft}$, Eq. (19), or alternatively $g_{\rm dc}^{\rm stim} = I^{\rm stim}/I_0^{\rm stim}$. However, in general the situation is much more complicated and a detail treatment of the full Boltzmann collision term is required, which will be left for a future publication.

4. Results for Wien spectra

4.1. Analytic expressions

For a Wien spectrum $n_{\rm W}(x) = N_0\,{\rm e}^{-x}$ of temperature θ_γ, with the condition $N_0 \ll \nu^2$, induced terms may be neglected. Above N_0 in physical units is defined by $N_{\gamma,0} = 8\pi\,N_0/c^3$, where $N_{\gamma,0}$ is the photon number density. Then the functions I_i are given by

$$
\begin{aligned}
I_{0,{\rm W}} &= 24\,N_0 && \text{(25a)}\\
I_{1,{\rm W}} &= -I_{0,{\rm W}}[21 - 6\rho]/\rho && \text{(25b)}\\
I_{2,{\rm W}} &= I_{0,{\rm W}}[428.4 - 220.5\rho + 15\rho^2]/\rho^2 && \text{(25c)}\\
I_{3,{\rm W}} &= -I_{0,{\rm W}}[9141.6 - 6854.4\rho \\
&\quad +1047.375\rho^2 - 11.25\rho^3]/\rho^3 && \text{(25d)}\\
I_{4,{\rm W}} &= I_{0,{\rm W}}[206380.8 - 205686\rho + 51408\rho^2 \\
&\quad -2480.625\rho^3 - 11.25\rho^4]/\rho^4\,. && \text{(25e)}
\end{aligned}
$$

Here we defined the ratio of the electron to photon temperature as $\rho = T_e/T_\gamma$. Making use of (22a) and (22b) one finds:

$$I_{\rm W}^{\rm inv} = \frac{24\,N_0}{1 + [21 - 6\rho]\;\theta_\gamma}\cdot \tag{26}$$

Here we replaced the electron temperature by $\theta_e \to \rho\,\theta_\gamma$.

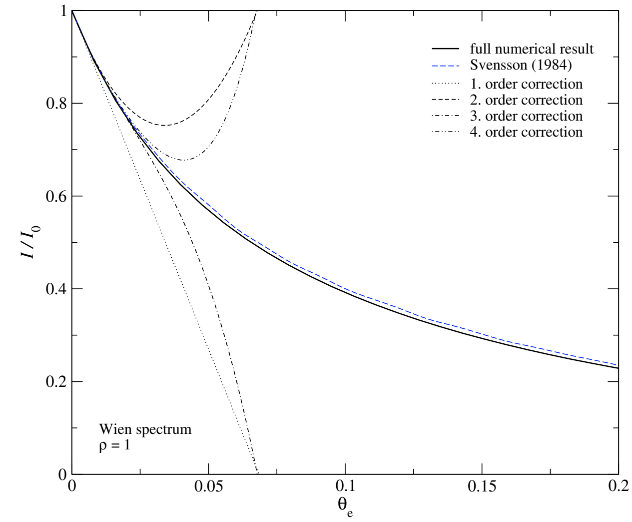

Fig. 5. DC soft photon production rate relative to the DC production rate I_0 as given by the Lightman-Thorne approximation as a function of the electron temperature $\theta_e = T_e/m_e$. All the curves were computed for initial photons with a Wien spectrum at temperature $T_\gamma \equiv T_e$. The full numerical results are shown in comparison with the *direct* expansion as given by equations (25) including temperature corrections up to different orders, as indicated. In addition, the approximation formula (27) as given by Svensson (1984) is shown. The approximations based on formulae (20) and (26) show a similarly good performance but for clarity are not presented here. For further discussion about the performance of the various approximations see Sect. 4.3.

4.2. Comparison with numerical results

4.2.1. Case $T_e = T_\gamma$

In Fig. 5 the results obtained for incoming Wien spectra with effective temperature $\theta_\gamma = \theta_e$ are shown. With increasing temperature the effective DC correction factor decreases strongly in both cases. This implies that for higher temperatures the efficiency of DC emission is significantly overestimated by the result obtained by Lightman (1981) and Thorne (1981). For example, even at moderate temperatures $T_e \sim 4$ keV there is a 10% negative correction due to higher order corrections in the energies of the initial photons and electrons. Since $I/I_0 < 1$, with Eq. (15) one can estimate that the main contribution to I has to come from photons with energies $\omega_0 \gtrsim \frac{10}{7}\,\theta_e$.

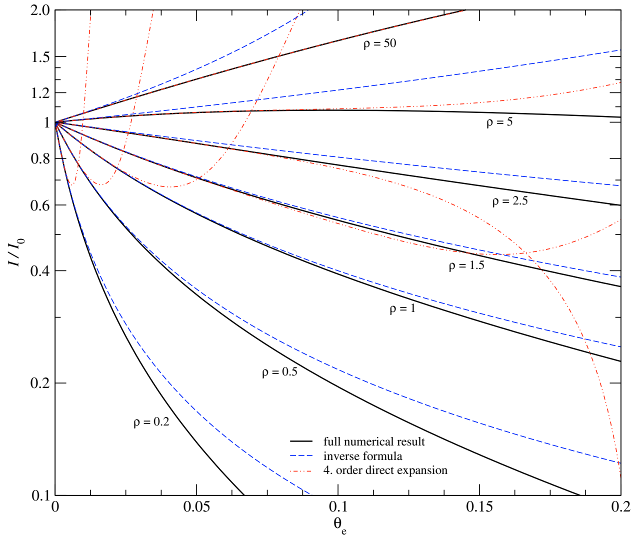

Fig. 6. DC soft photon production rate relative to the DC production rate I_0 as given by the Lightman-Thorne approximation as a function of the electron temperature $\theta_\mathrm{e} = T_\mathrm{e}/m_\mathrm{e}$. All the curves were computed for initial photons with a Wien spectrum at temperature T_γ and different values of $\rho = T_\mathrm{e}/T_\gamma$. The full numerical result, the fourth order direct formula as given by Eq. (25) and the inverse formula from Eq. (26) are given.

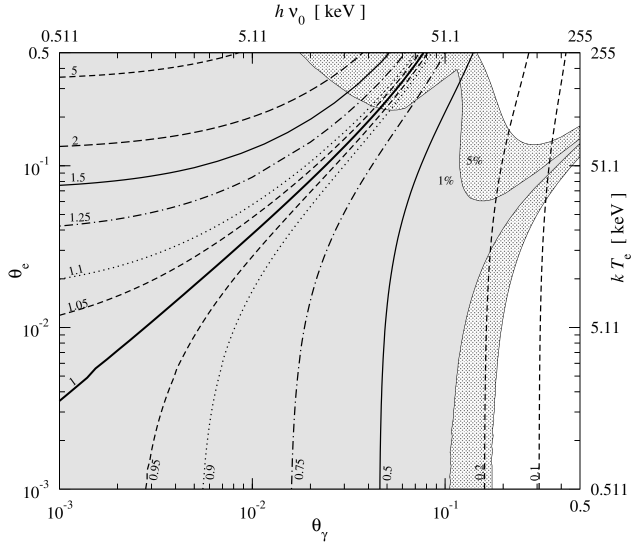

Fig. 7. DC emission correction factor for Wien spectra. The lines indicate the contours of I/I_0 = const as obtained by full numerical integrations. Within the shaded regions the approximation (20) is accurate to better than 1% and 5%, as indicated.

In the considered case the direct formulae (21) in fourth order of the electron temperature with (25) are valid up to $\theta_\mathrm{e} \sim 0.05$, within reasonable accuracy. As mentioned above the convergence of these asymptotic expansions is very slow. However, as will be shown below, the inverse formula (22a) and the corresponding coefficients a for $\rho \sim 1$ provide an approximation which is better than 5% up to $\theta_\mathrm{e} \sim 0.2$. Comparing the result for an incoming Wien spectrum with the approximation given by Svensson (1984),

$$I_\mathrm{S}(\theta_\mathrm{e}) \approx \frac{I_{0,\mathrm{W}}}{1 + 13.91\,\theta_\mathrm{e} + 11.05\,\theta_\mathrm{e}^2 + 19.92\,\theta_\mathrm{e}^3} \tag{27}$$

shows that for $\rho = 1$ Eq. (27) provides a very good fit to the full numerical results. The approximations based on formulae (20) and (26) show a similarly good performance. However, in the more general case, i.e. $\rho \neq 1$, the approximation given by Svensson (1984) does not reproduce the numerical results, since the strong dependence of the higher order corrections on the ratio of the electron to the photon temperature was not taken into account.

4.2.2. Case $T_\mathrm{e} \neq T_\gamma$

Figure 6 illustrates the dependence of the effective DC correction factor on the ratio of the electron to the photon temperature $\rho = T_\mathrm{e}/T_\gamma$ for an initial Wien spectra. In general the characteristics of the ratio I/I_0 can be summarized as follows: If we define the critical ratio $\rho_\mathrm{c} = 7/2 \sim 2.33$ of electron to photon temperatures, for which the first order correction to I vanishes (cf. Eq. (25b)), then two regimes can be distinguished: (i) for $\rho \lesssim \rho_\mathrm{c}$ the ratio I/I_0 monotonically decreases with increasing electron temperature; whereas (ii) for $\rho \gtrsim \rho_\mathrm{c}$ it first increases and then turns into a decrease at high temperature. This suggests that ρ_c separates the regions where Doppler boosting is compensating the suppression of DC emission due to higher photon energy. Estimating the mean photon energy weighted by I_0, i.e. $\langle\omega_0\rangle = \theta_\gamma \int x^5 n\,\mathrm{d}x / \int x^4 n\,\mathrm{d}x \approx 5\,\theta_\gamma$, and using $\omega_0 \sim \frac{10}{7}\,\theta_\mathrm{e}$ for the condition $G_\mathrm{m}(\omega_0, \theta_\mathrm{e}) = 1$ (see Eq. (15)) yields $\rho_\mathrm{c} \approx 7/2$, which further supports this conclusion.

In general one finds (see Figs. 6) that for $\rho < \rho_\mathrm{c}$ the *inverse* approximation (22a) has a better performance than the *direct* expansion formula (21) and vice versa for the case $\rho \geq \rho_\mathrm{c}$. The direct formula performs very well for $\rho \geq \rho_\mathrm{c}$ even in lower orders of the temperature corrections. Combining these two approximations an accuracy of better than ~5% can be achieved over a very broad range of temperatures. If the photons and electrons have similar temperatures, then the inverse formula (22a) is valid even up to $kT \sim 100$ keV. In Sect. 4.3 we discuss the range of applicability for the various approximations given above in more detail.

In Fig. 7 the dependence of the DC emission correction factor on the temperature of the initial photons and the temperature of the electrons is illustrated for Wien spectra. The Lightman-Thorne approximation is accurate in a very limited range of photon energies and electron temperatures. On the other hand, the approximation (20) works in practically the full considered range with very high accuracy. In contrast to the case of monoenergetic initial photons even at low temperatures of the photons the electrons have to be several times hotter in order to reach $I/I_0 = 1$. As discussed above this is due to the fact that the main emission is coming from photons with $\omega_0 >$ few $\times\,\theta_\gamma$.

4.3. Range of applicability for the different approximations

In the previous sections we have derived different kinds of analytic approximations for the DC emission coefficient. Each has advantages and disadvantages. For example the approximation (20) involves a 2-dimensional integral over the photon spectrum and the electron distribution, which is numerically more expensive than the 1-dimensional integrals for the direct expansion (21) or the inverse approximation (22). One obvious advantage of the inverse formula (22) over the direct expansion (21) is that only the first order corrections are needed to obtain an excellent approximation up to fairly high temperatures. Especially for numerical applications this is important, since higher order derivatives of the spectrum may lead to significant difficulties.

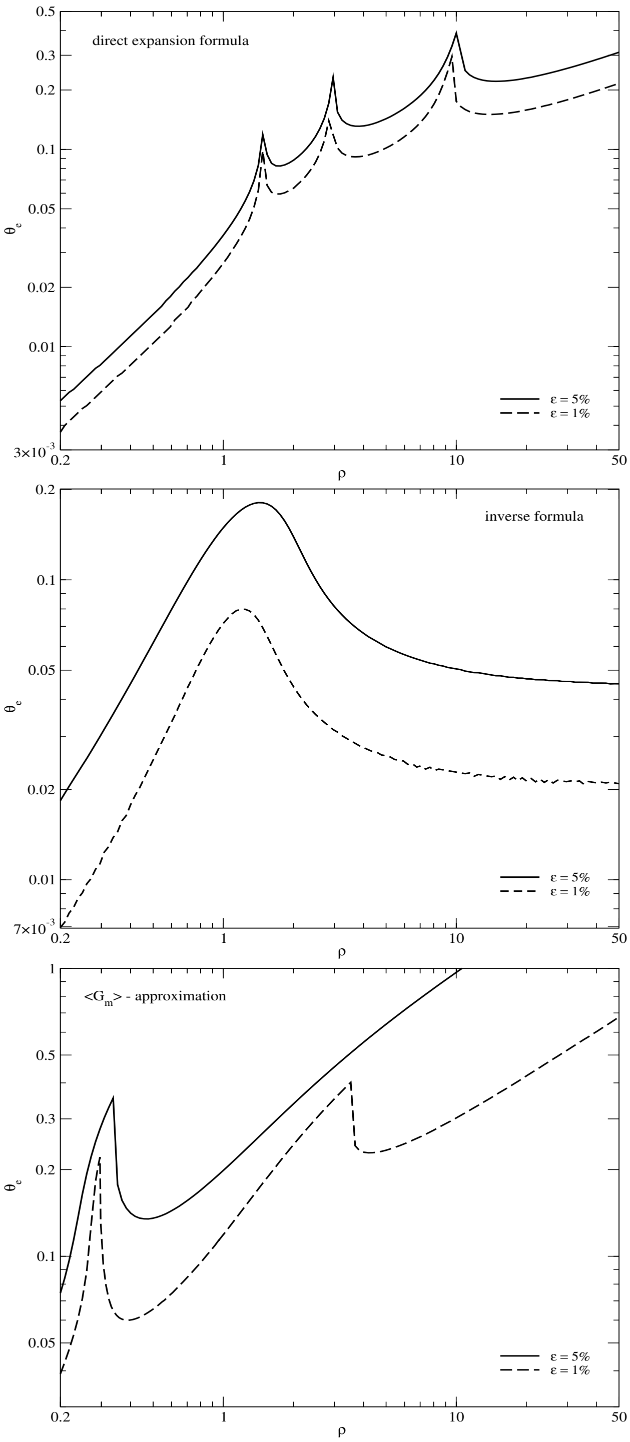

Fig. 8. Range of applicability for Wien spectra and different $\rho = T_e/T_\gamma$: the electron temperature θ_e is shown above which the relative difference between the considered analytic prediction and the numerical results becomes greater than ϵ. The numerical results were compared with the approximation (20), the *direct* expansion (21) up to fourth order in temperature and the *inverse* formula as given by Eq. (22).

However, it is necessary to investigate the range of applicability of each of these approximations in more detail.

We have studied the accuracy of these approximations for Wien spectra more extensively. For this purpose we have compared the different approximations with the results of the full numerical computation and, for a given $\rho = T_e/T_\gamma$, determined the lowest values of the electron temperature θ_e at which the approximation deviates by more than ϵ from the numerical results. In Fig. 8 we illustrate the outcome of these calculations for the approximation (20) based on the results for the monochromatic case, the *direct* expansion (21) up to fourth order in temperature and the *inverse* formula from Eq. (22). The peaks in the curves for the direct expansion (21) and approximation (20) appear where the relative difference to the results of the full computation in each case changes sign. For $\rho \lesssim 1$ the direct expansion breaks down very fast, while for $\rho \gtrsim 1$ it works very well. The inverse formula works best for cases close to $\rho = 1$. Whenever induced effects are negligible the approximation based on the results obtained for the monochromatic case is excellent, in particular for $\rho \gtrsim 1$.

5. Implications for the thermalization of spectral distortions of the CMB in the early Universe

In the high redshift Universe ($z \gtrsim 2.9 \times 10^5$) injection of energy into the medium leads to a residual μ-type distortion of the CMB today (Sunyaev & Zeldovich 1970; Illarionov & Sunyaev 1975a,b; Danese & de Zotti 1982; Burigana et al. 1991; Hu & Silk 1993b). In this case the photon occupation number can be expressed as $n(\nu) = 1/[e^{h\nu/kT_\gamma+\mu} - 1]$, with the dimensionless chemical potential μ, which in general is a function of frequency ν. At low frequencies ($h\nu \lesssim$ few $\times\, 10^{-3}kT_\gamma$) the production of soft photons by the DC process returns the photon distribution to a Planck spectrum after a very short time, whereas at high frequencies ($h\nu \gtrsim 0.1kT_\gamma$) very few photons are newly emitted and Compton scattering is only able to establish a Bose-Einstein spectrum with constant chemical potential. Therefore the time evolution of the high frequency spectrum depends critically on the rate at which soft photons are created by the DC process and then up-scattered by electrons via the Compton process.

The current limits on deviations of the CMB spectrum from a pure blackbody as obtained with COBE (Fixsen et al. 1996; Fixsen & Mather 2002) constrain the chemical potential today to obey $|\mu| < 9 \times 10^{-5}$, but this small residual distortion could have arisen from a huge energy injection at sufficiently high redshifts ($z \gtrsim 10^6$–10^7), where until today the resulting spectral distortions were washed out by the combined action of DC soft photon production and Comptonization.

Due to Compton scattering at these early stages the temperature of the electrons is always very close to the Compton equilibrium temperature in the given radiation field. For a μ-type distortion with $\mu \ll 1$ the difference between the radiation and electron temperature is small and hence for estimates of the DC emission coefficient one may assume $T_e \sim T_\gamma$. For small values of μ it is also sufficient to assume that the initial photon distribution is *very close* to a pure blackbody. As explained in Sect. 3.2 stimulated DC emission will only affect the effective DC correction factor at the percent level. With $n(x) = 1/[e^x - 1]$ and Eq. (22) $g_{dc}^{soft} \approx 1/[1 + 14.6\,\theta_\gamma]$, which implies that at high redshifts the thermalization of CMB spectral distortions will be less efficient, since the DC photon production rate is reduced compared to the Lightman-Thorne formula. For a temperature of $kT_\gamma \sim 4$ keV, higher order corrections lower the DC emissivity by $\sim$10%. This temperature corresponds to a redshift of roughly $z \sim 10^7$. Therefore one can expect that quantum-electrodynamical effects lead to significant corrections of the DC photon production rate for large energy injection at redshifts $z \gtrsim$ few $\times\, 10^6$. In addition, higher order temperature corrections to the Compton process may also lower the thermalization efficiency. This then will make the constraints placed on energy injection due to exponentially decaying relict particles with short lifetimes ($t_X \lesssim$ few $\times 10^6$ s) tighter and may affect the results obtained within the standard treatment (Hu & Silk 1993a) at a level ∼10%. However, a more detailed computation is beyond the scope of this work.

Higher order corrections to the DC process are negligible for the theoretical computations of y-type distortions (Zeldovich & Sunyaev 1969; Sunyaev & Zeldovich 1970; Illarionov & Sunyaev 1975a,b; Danese & de Zotti 1982; Burigana et al. 1991; Hu & Silk 1993b), since these only arise after energy release in the low redshift ($z \lesssim 10^4$) Universe, where not only the temperature has become very small, but also Bremsstrahlung dominates over DC emission.

6. Conclusion

Double Compton emission in an isotropic, mildly relativistic thermal plasma was investigated within the soft photon limit. Simple and accurate analytic expression for the low frequency DC emission coefficient have been derived, which extend the Lightman-Thorne approximation up to mildly relativistic temperatures of the medium and should be applicable in a broad range of physical situations. In particular, expressions for initially monochromatic photons and Wien spectra were given and discussed in detail.

It has been shown that the DC emissivity strongly decreases with higher mean energy of the initial photons leading to a suppression of the total number of newly created photons compared to the Lightman-Thorne approach. On the other hand increasing the temperature of the electrons leads to an enhancement of the DC emissivity. If the photons and the electrons have similar temperatures, which is the case in most physical situations close to full thermodynamic equilibrium, then formulae (22) should be applicable up to $kT \sim 100$ keV with an accuracy of better than a few percent. Since only first order corrections are necessary for this approximation, it is generally most suitable for numerical applications.

We also discussed possible consequences for the theoretical computations of the thermalization of μ-type CMB spectral distortions at high redshifts ($z \gtrsim$ few $\times 10^6$) and found that the new approximations could change the results at the level of a few percent, possibly up to ∼10%. However, these corrections are currently beyond the reach of observational possibilities.

Acknowledgements. We would like to thank the anonymous referee for comments.

Appendix A: Expansion of the relativistic Maxwell Boltzmann distribution

The low temperature expansion of (3) leads to

$$
\begin{aligned}
f(E) = \frac{N_{\rm e}\, e^{-\xi}}{(2\pi\, m_{\rm e}^6\, \theta_{\rm e})^{3/2}} \Bigg[& 1 - \theta_{\rm e} \cdot \left(\frac{15}{8} - \frac{1}{2}\xi^2\right) \\
& + \theta_{\rm e}^2 \cdot \left(\frac{345}{128} - \frac{15}{16}\xi^2 - \frac{1}{2}\xi^3 + \frac{1}{8}\xi^4\right) \\
& - \theta_{\rm e}^3 \cdot \left(\frac{3285}{1024} - \frac{345}{256}\xi^2 - \frac{15}{16}\xi^3 - \frac{25}{64}\xi^4 + \frac{1}{4}\xi^5 - \frac{1}{48}\xi^6\right) \\
& + \theta_{\rm e}^4 \cdot \left(\frac{95355}{32768} - \frac{3285\,\xi^2}{2048} - \frac{345\,\xi^3}{256} - \frac{855\,\xi^4}{1024} - \frac{13\,\xi^5}{32} \right. \\
& \left. + \frac{51\,\xi^6}{128} - \frac{\xi^7}{16} + \frac{\xi^8}{384}\right) \Bigg], \qquad \text{(A.1)}
\end{aligned}
$$

with $\xi = \eta^2/2\,\theta_{\rm e}$ and $\eta = p/m_{\rm e}$.

Appendix B: Squared matrix element for double Compton

For the DC differential cross section one has to calculate the squared matrix element $|\mathcal{M}|^2 = e^6\, X$ describing the DC process. This calculation was first performed by Mandl & Skyrme (1952). In Jauch & Rohrlich (1976) one can find the expression for the squared matrix element of the double Compton process (p. 235):

$$
\begin{aligned}
X = {} & 2\,(a\,b - c)\Big[(a+b)(2+x) - (a\,b - c) - 8\Big] - 2\,x\Big[a^2 + b^2\Big] \\
& -2\,[a\,b + c\,(1-x)]\,\rho \\
& -8\,c + \frac{4\,x}{A\,B}\Bigg[(A+B)\,(1+x) + x^2\,(1-z) \\
& +2\,z - (a\,A + b\,B)\left(2 + \frac{(1-x)\,z}{x}\right)\Bigg], \qquad \text{(B.1)}
\end{aligned}
$$

where the following abbreviations have been used

$$
\begin{aligned}
a &= \frac{1}{\kappa_0} + \frac{1}{\kappa_1} + \frac{1}{\kappa_2} \\
b &= \frac{1}{\kappa_0'} + \frac{1}{\kappa_1'} + \frac{1}{\kappa_2'} \\
c &= \frac{1}{\kappa_0\,\kappa_0'} + \frac{1}{\kappa_1\,\kappa_1'} + \frac{1}{\kappa_2\,\kappa_2'} \qquad \text{(B.2a)}
\end{aligned}
$$

$$
\begin{aligned}
x &= \kappa_0 + \kappa_1 + \kappa_2 \\
z &= \kappa_0\,\kappa_0' + \kappa_1\,\kappa_1' + \kappa_2\,\kappa_2' \qquad \text{(B.2b)}
\end{aligned}
$$

$$
\begin{aligned}
A &= \kappa_0\,\kappa_1\,\kappa_2 \\
B &= \kappa_0'\,\kappa_1'\,\kappa_2' \\
\rho &= \frac{\kappa_0}{\kappa_0'} + \frac{\kappa_0'}{\kappa_0} + \frac{\kappa_1}{\kappa_1'} + \frac{\kappa_1'}{\kappa_1} + \frac{\kappa_2}{\kappa_2'} + \frac{\kappa_2'}{\kappa_2}. \qquad \text{(B.2c)}
\end{aligned}
$$

For the definitions of κ_i, κ_i' we used those of the original paper from Mandl & Skyrme (1952):

$$
\begin{aligned}
m_{\rm e}^2\,\kappa_0 &= -P\cdot K_0 \quad m_{\rm e}^2\,\kappa_1 = +P\cdot K_1 \quad m_{\rm e}^2\,\kappa_2 = +P\cdot K_2 \qquad \text{(B.3a)} \\
m_{\rm e}^2\,\kappa_0' &= +P'\cdot K_0 \quad m_{\rm e}^2\,\kappa_1' = -P'\cdot K_1 \quad m_{\rm e}^2\,\kappa_2' = -P'\cdot K_2, \qquad \text{(B.3b)}
\end{aligned}
$$

with the standard signature of the Minkowski-metric $(+ - - -)$. Assuming that the outgoing photon $\gamma(K_2)$ is *soft* compared to $\gamma(K_1)$ one can expand X into orders of the frequency ω_2 and keep only the lowest order term, i.e. terms of the order $O(\omega_2^{-2})$. Similar expansions for the limits $\omega_0 \ll 1$ and $\beta \ll 1$ can be performed. Since the results of these expansions are extremely complex and not very useful, we have omit them here.

Appendix C: Numerical solution of the Boltzmann integrals

To solve the Boltzmann integrals we implemented two different programs, one based on the NAG routine `D01GBF`, which uses an adaptive Monte-Carlo method to solve multidimensional integrals, the other using the VEGAS routine of the CUBA Library[4] (Hahn 2004). The latter turned out to be much more efficient as it

[4] Download of the CUBA Library available at: `http://www.feynarts.de/cuba/`

significantly benefitted from importance sampling. The expense and performance of the calculation critically depend on the required accuracy. For most of the calculations presented here we chose a relative error of the order of $\epsilon \sim 10^{-3}$. For the integrations over different initial photon distributions we typically used $\omega_{\rm min} = 10^{-4}\,\theta_\gamma$ and $\omega_{\rm max} = 25\,\theta_\gamma$.

Integration over the electron momenta

In order to restrict the integration region over the electron momenta for low electron temperature we determined the maximal Lorentz factor, $\gamma_{\rm max}$, such that the change in the normalization of the electron distribution was less than a fraction of the required accuracy. Instead of p we used the variable $\xi = \eta^2/2\,\theta_{\rm e}$ with $\eta = p/m_{\rm e}$.

For high electron temperature it turned out to be more efficient to use the normalization of the electron distribution itself as a variable. For this we defined

$$N(x) = m_{\rm e}^3 \int_1^x \gamma\,\sqrt{\gamma^2-1}\,f(\gamma m_{\rm e})\,{\rm d}\gamma\,, \tag{C.1}$$

which for $x \to \infty$ becomes $N \equiv N_{\rm e}$. In actual calculations one has to invert this equation to find the function $x(N)$. This was done numerically before the integrations were performed for a sufficiently large number of points ($n \sim 512$) such that the function $x(N)$ during the integrations could be accurately represented via spline interpolation. Here it is important to bear in mind, that $N(x)$ is rather steep for $x \sim 0$ and $x \sim 1$.

C.1. Definition of I_k

Inserting the direct expansion of $G_{\rm m}$ in low energies of the initial photon and electron temperature Eq. (15) into Eq. (20) and collecting the different orders in $\theta_{\rm e}$, one can define the functions I_i of Eq. (21) as

$$I_0 = \mathcal{D}_4 \tag{C.2a}$$

$$I_1 = 6\,\mathcal{D}_4 - \frac{21}{5}\frac{\theta_\gamma}{\theta_{\rm e}}\mathcal{D}_5 \tag{C.2b}$$

$$I_2 = 15\,\mathcal{D}_4 - \frac{441}{10}\frac{\theta_\gamma}{\theta_{\rm e}}\mathcal{D}_5 + \frac{357}{25}\left[\frac{\theta_\gamma}{\theta_{\rm e}}\right]^2\mathcal{D}_6 \tag{C.2c}$$

$$I_3 = \frac{45}{4}\mathcal{D}_4 - \frac{8379}{40}\frac{\theta_\gamma}{\theta_{\rm e}}\mathcal{D}_5 + \frac{5712}{25}\left[\frac{\theta_\gamma}{\theta_{\rm e}}\right]^2\mathcal{D}_6 - \frac{7618}{175}\left[\frac{\theta_\gamma}{\theta_{\rm e}}\right]^3\mathcal{D}_7 \tag{C.2d}$$

$$I_4 = -\frac{45}{4}\mathcal{D}_4 - \frac{3969}{8}\frac{\theta_\gamma}{\theta_{\rm e}}\mathcal{D}_5 + \frac{8568}{5}\left[\frac{\theta_\gamma}{\theta_{\rm e}}\right]^2\mathcal{D}_6 - \frac{34281}{35}\left[\frac{\theta_\gamma}{\theta_{\rm e}}\right]^3\mathcal{D}_7 + \frac{21498}{175}\left[\frac{\theta_\gamma}{\theta_{\rm e}}\right]^4\mathcal{D}_8\,, \tag{C.2e}$$

where we introduce the integrals $\mathcal{D}_i$ as

$$\mathcal{D}_i = \int x^i\,n\,{\rm d}x \tag{C.3}$$

over the initial photon distribution $n(\nu)$.

References

Abramovitz, M., & Stegun, I. A. 1965 (Inc. New York: Dover Publications)
Burigana, C. Danese, L., & de Zotti, G. 1991, A&A, 246, 49
Danese, L., & de Zotti, G. 1982, A&A, 107, 39
Fixsen, D. J., & Mather, J. C. 2002, ApJ, 581, 817
Fixsen, D. J.,Cheng, E. S., Gales, J. M., et al. 1996, ApJ, 473, 576
Gould, R. J. 1984, ApJ, 285, 275
Hahn, T. 2004, hep-ph/0404043, download of the CUBA Library available from: http://www.feynarts.de/cuba/
Hu, W., & Silk, J. 1993a, Phys. Rev. Lett., 18, 2661
Hu, W., & Silk, J. 1993b, Phys. Rev. D, 48, 485
Illarionov, A. F., & Sunyaev, R. A. 1975a, Sov. Astron., 18, 413
Illarionov, A. F., & Sunyaev, R. A. 1975b, Sov. Astron., 18, 691
Jauch, J. M., & Rohrlich, F. 1976, Springer-Verlag
Lightman, A. P. 1981, ApJ, 244, 392
Mandl, F., & Skyrme, T. H. R. 1952, Proc. Roy. Soc., A215, 497
Pozdnyakov, L. A., Sobol, I. M., & Sunyaev, R. A. 1983, Astrophys. & Space Phys. Rev., ed. R. A. Sunyaev (Harwood Academic Publishers), Chur, 2, 189
Svensson, R. 1984, MNRAS, 209, 175
Sunyaev, R. A., & Zeldovich, Ya. B. 1970, Ap&SS, 7, 20
Thorne, K. S. 1981, MNRAS, 194, 439
Zeldovich, Y. B., & Sunyaev, R. A. 1969, Ap&SS, 4, 301